ELSEVIER

Chemical Engineering Journal 84 (2001) 491–496

Chemical Engineering Journal

www.elsevier.com/locate/cej

Particle transport by jet pump in a new liquid–solid circulating moving bed reactor

Minghan Han*, Cong Xu, Jinfu Wang, Sheng Chen, Yong Jin

Department of Chemical Engineering, Tsinghua University, Beijing 100084, PR China

Received 25 April 2000; received in revised form 1 November 2000; accepted 6 November 2000

Abstract

The liquid–solid circulating moving bed reactor is a novel one, which consists of two or more reaction chambers and a particle transport system. Particles move down to the lower reaction chamber from the upper reaction chamber through an upper conduit and to the particle transport system through a lower conduit, and then are conveyed into the upper reaction chamber through a riser. The renewing speed of particles in the reaction chamber is determined by the circulating rate of particles, which is one of the key factors in the operation of the reactor. Three different kinds of auxiliary liquids are used to regulate the circulating rate of particles, and a suitable configuration of particle transport system is established. A model of particle transport based on mass, momentum and energy balance is proposed and used for simulation of the process. © 2001 Elsevier Science B.V. All rights reserved.

Keywords: Moving bed reactor; Particle; Transport; Jet pump

1. Introduction

In industry, there are many processes, such as reaction–regeneration, reaction–reaction and adsorption–desorption, where solid particles (catalysts or adsorbents) are recirculated. When the particle size of solid catalysts is big and the catalysts have to stay for a relative long period in the reactor, circulating fluidized bed reactors usually cannot meet the technological requirements for liquid–solid catalytic reactions. For this reason, a liquid–solid circulating moving bed reactor [1], suitable for use in a reaction–regeneration coupled system, has been developed and applied to the synthesis of linear alkylbenzenes (LAB) catalyzed by solid acid catalyst.

LAB are valuable industrial chemicals used in the manufacture of detergents. These are usually mixtures of C_9–C_{14} alkylbenzenes synthesized by the alkylation of benzene with mixed linear olefins using anhydrous HF as catalyst. Due to the hazardous nature of anhydrous HF, efforts have been made to find environmentally safer catalysts like solid acid catalyst [2–7]. The disadvantage of the solid acid catalyst is that it is easily deactivated because the by-products are gum-polymers and tend to accumulate on the surface of the catalyst and block reactive sites. Fortunately, the deactivating material agent can readily be desorbed from the catalyst by washing the catalyst with the aromatic reactant.

The UOP Detal process [8–13], is an example of the green production technology of LAB. As the deactivation rate of solid acid catalysts is rather fast, two fixed bed reactors are employed in this technology for the operation of reaction and regeneration alternatively, using a 24 h switch cycle. Even so, it is inconvenient for this operation to be used industrially because of its discontinuous nature. The liquid–solid circulating moving bed reactor can couple the processes of reaction and regeneration and avoid the above inconvenience by enabling the catalyst to circulate continuously in the system.

The renewing rate of the solids in the reaction chamber depends on the circulating rate of particles, and is thus, very important for the operation of the system. In this paper, therefore, the particle transport in the reactor is studied systematically for better understanding the mechanism of particle circulation.

2. Experimental apparatus and methods

The experimental set-up of the liquid–solid circulating moving bed reactor is shown in Fig. 1, which is a cold model for the synthesis of LAB. The sizes of the regeneration chamber B and the reaction chamber D are 90 mm(i.d.) × 800 mm (length) and 65 mm × 800 mm, respectively. The dimension of the upper conduit C, the lower conduit E and the riser

* Corresponding author. Tel.: +86-10-6278-8984; fax: +86-10-6277-2051.
E-mail address: hanmh@ihw.com.cn (M. Han).

1385-8947/01/$ – see front matter © 2001 Elsevier Science B.V. All rights reserved.
PII: S1385-8947(00)00372-7

Nomenclature

C	structural parameter, $(f_2-f_1)/f_{S1}$
C_{Q_5}	the concentrations of ethanol in Q_5
$C_{sampling}$	the concentrations of the sampling
D	diameter (m)
f_1	area of nozzle (m^2)
f_2	area of cross-section 2×2 m^2
f_{Sl}	area of the annular space of the curved-section 1×1 (m^2)
f_x	wall surface area in jet-flow zone of suction chamber (m^2)
m	configuration parameter, f_2/f_1
M	mass flowrate ($kg\,s^{-1}$)
n	configuration parameter, f_2/f_{S1}
P	pressure ($N\,m^{-2}$)
Q	volume flowrate ($m^3\,s^{-1}$)
Q_1	outlet liquid flowrate in regeneration chamber ($m^3\,s^{-1}$)
Q_2	outlet liquid flowrate in reaction chamber ($m^3\,s^{-1}$)
Q_3	inlet liquid flowrate in reaction chamber ($m^3\,s^{-1}$)
Q_4	driving flowrate ($m^3\,s^{-1}$)
Q_5	outlet liquid flowrate in the separator ($m^3\,s^{-1}$)
Q_a, Q_I, Q_{II}, Q_{III}	auxiliary liquid flowrate ($m^3\,s^{-1}$)
Q_E	liquid flowrate in the lower conduit ($l\,h^{-1}$)
Q_{move}	liquid flowrate in the annular space of the cross-section 1×1 ($l\,h^{-1}$)
Q_S	particle-circulating rate ($l\,h^{-1}$)
Q_{S0}	particle-circulating rate without auxiliary liquid ($l\,h^{-1}$)
U	flow velocity ($m\,s^{-1}$)
Z	height of cross-section (m)

Greek letters

β	slope angle
ε	voidage
γ	volume weight ($kg\,m^{-2}\,s^{-2}$)
η	efficiency of auxiliary liquid
ρ	density ($kg\,m^{-3}$)
ξ	resistance coefficient

Subscripts

B	regeneration chamber
C	joint pipe
D	reaction chamber
E	lower conduit
F	riser
L	liquid
move	flow in the annular space of the curved-section 1×1
M	mixed fluid of liquid–solid
S	solid
1	curved-section 1×1
2	cross-section 3×2

F are 24 mm × 350 mm, 24 mm × 500 mm and 9 mm × 3000 mm, respectively. In the cold model experiments, water and ethanol are used instead of benzene and olefins as in hot model experiments. For the solid phase, variable color silica gel is used and its average particle diameter is 3.26 mm. The bulk density of the dry particles is $1027.8\,kg\,m^{-3}$, whereas the bulk density of the wet particles is $1227.8\,kg\,m^{-3}$. The measured voidage of the particles is 0.48.

The cold model experiment is conducted as follows: the reactants enter the reaction chamber D from the bottom inlet of the chamber, then go upward to contact catalyst particles counter-currently and the product is discharged through the upper outlet of the reaction chamber. The deactivated catalyst particles in the reaction chamber move downward and go into the suction chamber N through the lower conduit E

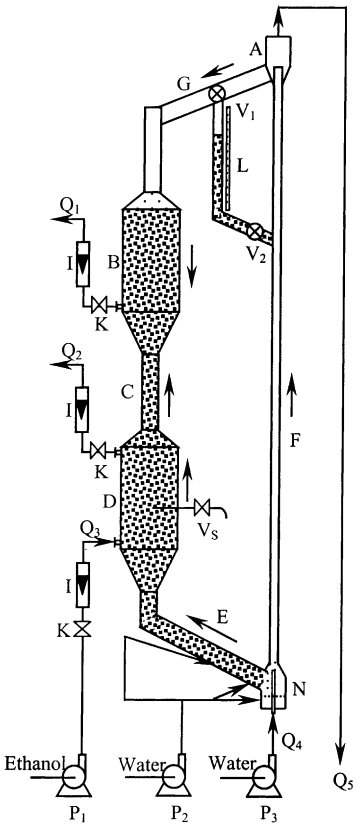

Fig. 1. Experimental apparatus of liquid–solid circulating moving bed reactor The direction of the arrows is that of the liquid flow in the reactor. Where A — separator, B — regeneration chamber, C — upper conduit, D — reaction chamber, E — lower conduit, F — riser, G — conduit between B and A, I — rotameter, K — regulator, L — gauge pipe, N — suction chamber, P_1–P_3 — pumps, Q_1–Q_5 — flowrate of liquid, V_1 and V_2 — butterfly valves, and V_S — sampling valve.

under the action of gravity. Then they are entrained by the driving flow Q_4 from the jet nozzle and conveyed into the liquid–solid separator A through the riser F. A fraction of the driving flow is used as regeneration liquid together with the particles enters the regeneration chamber B where the catalysts are regenerated, and the remainder is discharged through the liquid outlet of the separator. The regeneration liquid is discharged from the bottom outlet of the regeneration chamber and the regenerated catalysts move into the reaction chamber through the upper conduit C. Thus, a circulating operation of catalyst particles is realized.

In order to determine the particle-circulating rate quantitatively, a special device is designed and mounted to the system, which consists of a gauge pipe L and two butterfly valves V_1 and V_2. The butterfly valve V_1 is made of mesh and can only hold back the particles. By switching V_1, the particles can move into gauge pipe L instead of conduit G, the particle-circulating rate can be obtained by measuring the height change of the particles in the gauge pipe with respect to time. After the measurement has been done, V_1 is switched to make the particles to move only in conduit G and V_2 is opened to make the particles move into the riser.

In order to obtain the flowrate of liquid in the different parts of the reactor, the following combined equations are obtained from the principle of mass balance

$$Q_1 = Q_B + Q_C \tag{1}$$

$$Q_2 = Q_D - Q_C \tag{2}$$

$$Q_3 = Q_D - Q_E \tag{3}$$

$$Q_4 = Q_E + Q_F \tag{4}$$

Because the concentration of ethanol in riser F is equal to that in Q_5, when Q_E is negative

$$C_{Q_5} = \frac{-Q_E}{Q_4 - Q_E} \tag{5}$$

When Q_E is positive, the concentration of ethanol in the reaction chamber is

$$C_{\text{sampling}} = \frac{Q_3}{Q_E + Q_3} \tag{6}$$

In experiments, Q_1, Q_2, Q_3, and Q_4 are measured by rotameters, the concentrations of ethanol in Q_5 and the sampling from V_S are analyzed by gas chromatography (GC). The flowrates of liquids in the different parts of the reactor can be calculated from the above equations.

3. Results and discussion

3.1. Transport system

The circulating rate of particles Q_S in the reactor can be radically affected by the configuration of the transport system. A suitable transport system should be able to regulate the particle circulation over quite a large range under the condition of rather small liquid upflow in the lower conduit. Based on the principle of jet pumps [14], a configuration of suction chamber has been designed, as shown in Fig. 2. The driving flow Q_4 enters the reactor through the nozzle of the jet flow pipe O and forms a jet flow zone in the suction chamber N. Solid particles are sucked into the jet flow zone under the suction of the jet flow and are entrained upward. The jet flow pipe, the suction chamber and the riser jointly form the transport system for the particles.

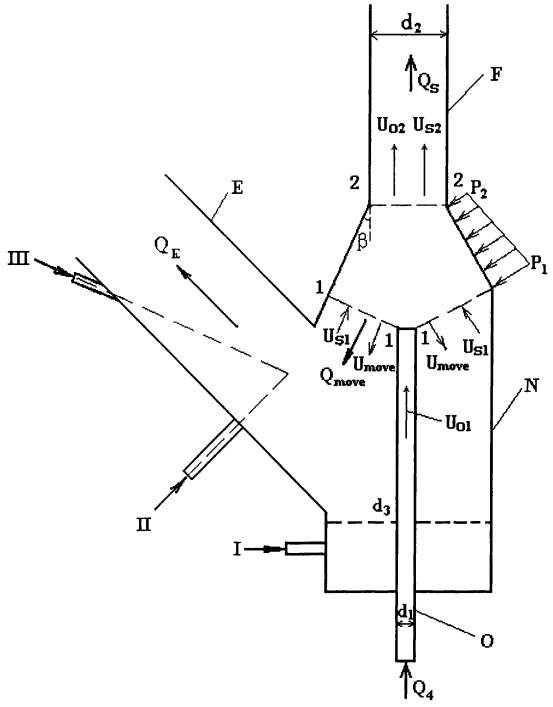

Fig. 2. The schematic diagram of the configuration of the jet transport I, II, III — auxiliary liquid, E — lower conduit, F — riser, N — suction chamber, O — jet flow pipe, Q_4 — flowrate of driving flow, Q_E — liquid flowrate in the lower conduit, Q_{move} — liquid flowrate in the annular space of the cross-section 1×1, $d_1 = 3$ mm, $d_2 = 9$ mm, $d_3 = 24$ mm, $\beta = 16^\circ$, L_c (the distance from the nozzle outlet to cross-section 3×2) $= 25$ mm.

To regulate the particle-circulating rate, auxiliary liquid flow I is conventionally used. According to our experimental observation, however, when only the auxiliary liquid I is used for regulation, the particles near the upper pipe wall of the lower conduit E will move quickly while those near the lower pipe wall will move slowly. Thus, the lower conduit is not fully used for particle transport. In order to raise the transport rate of particles, extra auxiliary liquid flows, II and III, are also added so as to push particles near the lower pipe wall to move down quickly. Therefore, three auxiliary regulation liquid streams, I, II and III, are present in the reactor, and we need to find the optimal design and its optimal operation conditions.

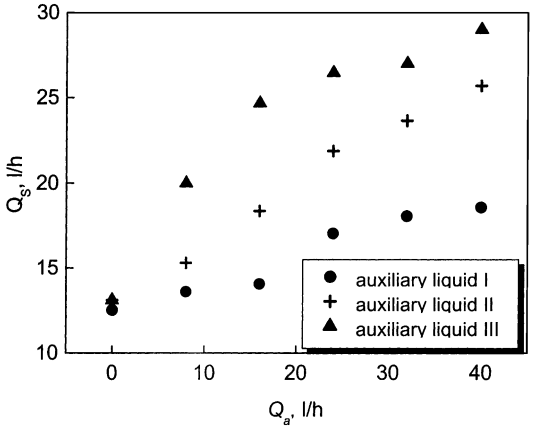

Fig. 3. Effect of auxiliary liquid on particle circulating rate.

3.2. Effects of the different auxiliary liquids on the particle-circulating rate and the liquid flowrate in the lower conduit

It can be seen from Figs. 3 and 4, that Q_S and Q_E vary rather greatly when each of the three different auxiliary liquid flows is used on its own. As the auxiliary liquid III can effectively improve the downward movement of the particles near the lower pipe wall of the lower conduit, the particle-circulating rate is the largest with the addition of the auxiliary liquid III. The effect of the auxiliary liquid II ranks second, and that of the conventional auxiliary liquid I appears to be least important. However, the auxiliary liquids can cause different effects on Q_E, the increase of Q_E caused by the auxiliary liquid III is the greatest, while that caused by the auxiliary liquid II is smaller. When the conventional auxiliary liquid I is used, Q_E is the smallest and even becomes negative. In this paper, the liquid flow direction in the lower conduit is defined as positive when it flows upward and negative when downward.

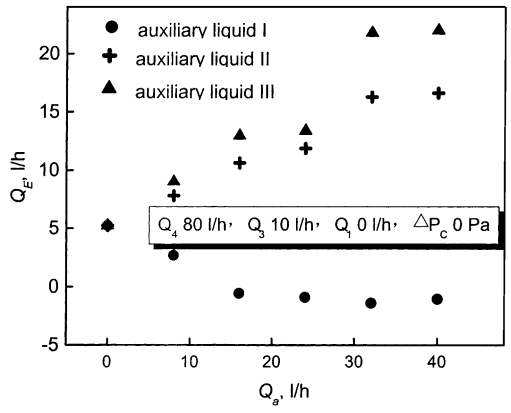

Fig. 4. Effect of auxiliary liquid on liquid flowrate in the lower conduit.

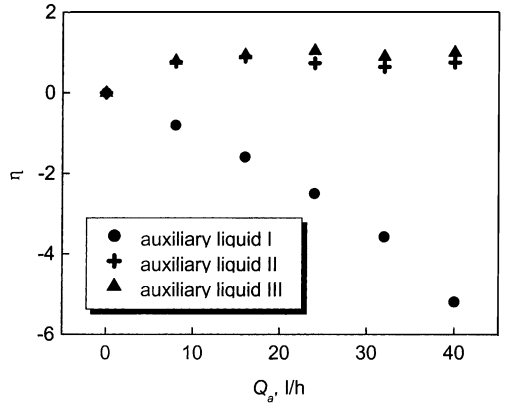

Fig. 5. Comparison of the efficiency of three different auxiliary liquids.

3.3. Comparison of the efficiency of the auxiliary liquids

In the operation of the liquid–solid circulating moving bed reactor, the particle circulation rate Q_S should be regulated within the range required for the synthesis of LAB. In addition, the liquid in the lower conduit must move upward to avoid that the reactants enter the particle transport system. However, if Q_E is too large, the molar ratio of benzene to olefins in the reactor will be changed significantly and unfavorable effects on the reaction will occur. This means that Q_E must be positive but at the same time cannot be too large. Therefore, for the synthesis of LAB, the optimum goal is to obtain a large particle circulation rate with the help of rather small upflow of liquid. For this reason, a quantitative factor η can be defined to determine the efficiency of the auxiliary liquid as follows:

$$\eta = \frac{(Q_S - Q_{S0})}{Q_E} \tag{7}$$

As shown in Fig. 5, the auxiliary liquid III and the auxiliary liquid II have almost the same efficiency. However, the auxiliary liquid III provides the higher particle-circulating rate, so it proves to be the most suitable flow of auxiliary liquid.

3.4. Transport model

As the efficiency of the auxiliary liquid III is the highest, for the transport model the auxiliary liquid flow III has been taken into account. To establish the transport model, we take the space formed from the curved surface 1×1, the cross-section 3×2 and the wall surface in jet-flow zone as a control volume shown in Fig. 2. Where Q_S is dependent on Q_4, Q_E, the pressure at the outlet of the jet flow pipe and the pressure at the cross-section 2×2. When the transport process is operated in a steady-state, the mass, momentum and energy balance can be established as follows, respectively.

3.4.1. Mass balance between curved surface 1×1 and cross-section 2×2

For solid flow

$$M_{S1} = M_{S2} \tag{8}$$

For liquid flow

$$M_{L2} = M_{L1} - M_{move} \tag{9}$$

where

$$Q_{move} = Q_E - Q_a \tag{10}$$

3.4.2. Momentum balance between curved surface 1×1 *and cross-section* 2×2

The accumulated momentum is zero in a stable state operation, so the momentum conservation equation can be established as

$$\begin{aligned}(M_{L1}U_{L1} &+ M_{S1}U_{S1}\cos\beta - M_{move}U_{move}\cos\beta)\\ &-(M_{L2}U_{L2} + M_{S2}U_{S2})\\ &= (P_2 + \gamma_2 Z_2) f_2 + \Delta P \sin\beta\, f_x\\ &-(P_1 + \gamma_1 Z_1)(f_{S1}\cos\beta + f_1)\end{aligned} \tag{11}$$

As shown in Fig. 2, $\Delta P \sin\beta f_x$ is the counter-force on wall surface [14].

$$\Delta P = (P_1 + \gamma_1 Z_1) f_2 + C[(P_2 + \gamma_2 Z_2) - (P_1 + \gamma_1 Z_1)] \tag{12}$$

where C is the distribution coefficient of counter-force, can be expressed as

$$C = \frac{(f_2 - f_1)}{f_{S1}} \tag{13}$$

and

$$f_x \sin\beta + f_2 = f_{S1}\cos\beta + f_1 \tag{14}$$

or

$$f_x = \frac{(f_{S1}\cos\beta + f_1 - f_2)}{\sin\beta} \tag{15}$$

Thus,

$$\begin{aligned}(M_{L1}U_{L1} &+ M_{S1}U_{S1}\cos\beta - M_{move}U_{move}\cos\beta)\\ &-[M_{L2}U_{L2} + M_{S2}U_{S2}]\\ &= [(P_2 + \gamma_2 Z_2) - (P_1 + \gamma_1 Z_1)]\\ &\times \left[f_2 + (f_2 - f_1)\cos\beta - \frac{(f_2 - f_1)^2}{f_{S1}} \right]\end{aligned} \tag{16}$$

3.4.3. Energy balance between the curved-section 1×1 *and the cross-section* 2×2

The energy balance can be established according to the Bernoulli equation on the assumption that the mixed fluid of liquid–solid is a homogeneous fluid. It reads

$$\begin{aligned}P_1 + \gamma_1 Z_1 + \rho_1 \frac{U_{M1}^2}{2}\\ = P_2 + \gamma_2 Z_2 + \rho_2 \frac{U_{M2}^2}{2} + \xi\rho_1 \frac{U_{M1}^2}{2}\end{aligned} \tag{17}$$

where

$$\begin{aligned}U_{M1} &= \frac{Q_M}{(f_1 + f_{S1})}, \quad U_{M2} = \frac{Q_M}{f_2},\\ Q_M &= Q_4 - Q_{move} + Q_S; \qquad \rho_1 = \varepsilon_1\rho_L + (1 - \varepsilon_1)\rho_S,\\ \rho_2 &= \varepsilon_2\rho_L + (1 - \varepsilon_2)\rho_S; \qquad \varepsilon_1 = \left(\frac{f_2}{f_{S1}}\right)\varepsilon_2,\\ \varepsilon_2 &= \frac{(Q_4 - Q_{move})}{(Q_4 - Q_{move} + Q_S)}\end{aligned}$$

and ξ is the resistance coefficient. Because the value of Q_s is rather small compared with Q_4, the quotient of $(Q_4 - Q_{move})/(Q_4 - Q_{move} + Q_s)$ equals 1 approximately. Furthermore, the value of $\cos\beta$ tends to 1 due to β being rather small. Introducing the structural parameters, $m = f_2/f_1$ and $n = f_2/f_{S1}$ and combining Eqs. (8), (9), (16) and (17), the transport model can be obtained as follows:

$$\begin{aligned}Q_S &= \frac{n-1}{2n}\\ &\times \left\{ \left[(Q_4 - Q_{move})^2 + \frac{4n}{n-1} S \right]^{1/2} - (Q_4 - Q_{move}) \right\}\end{aligned} \tag{18}$$

where

$$\begin{aligned}S &= \frac{\rho_L}{\rho_S}[mQ_4^2 - Q_{move}^2 - (Q_4 - Q_{move})^2]\\ &-\frac{1}{2}(Q_4 - Q_{move})^2 \left[1 + \frac{m-1}{m} - \frac{n}{m^2}(m-1)^2 \right]\\ &\times \left\{ (1 - \xi) \left[\frac{\rho_L}{\rho_S} m^2 n + m^2(1 - n) \right] - \frac{\rho_L}{\rho_S} \right\}\end{aligned} \tag{19}$$

The particle-circulating rate, Q_S, can be calculated from Eq. (18) according to the known equipment and operating parameters. In addition, Eq. (18) shows an explicit relationship between the particle-circulating rate and these parameters. It can be seen from Eq. (18), for example, that Q_S will increase with the growth of Q_4 and the decrease of Q_E.

3.5. Estimating parameter ξ *and verification of the model*

3.5.1. Resistance coefficient ξ

The parameter ξ can be estimated by fitting the experimental data with the mathematical model. For the case of absence of auxiliary liquid, $Q_{move} = Q_E$, $Q_F = Q_4 - Q_{move} \approx Q_4$, we obtain

$$\xi = 0.898 - 0.208\frac{Q_E}{Q_4} - 0.094\left(\frac{Q_E}{Q_4}\right)^2 \tag{20}$$

and for the case of presence of auxiliary liquid, $Q_{move} = Q_E - Q_{III}$, $Q_F = Q_4 - Q_{move} \approx Q_4$, we obtain

$$\xi = 0.941 - 0.113\frac{Q_E - Q_{III}}{Q_4} \tag{21}$$

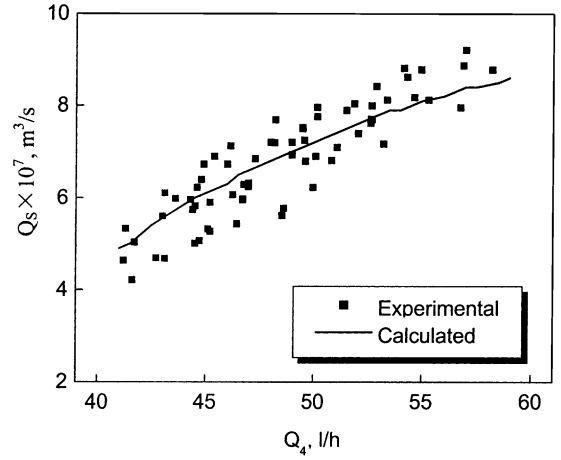

Fig. 6. Comparison of simulation data with experimental data when there is no auxiliary liquid.

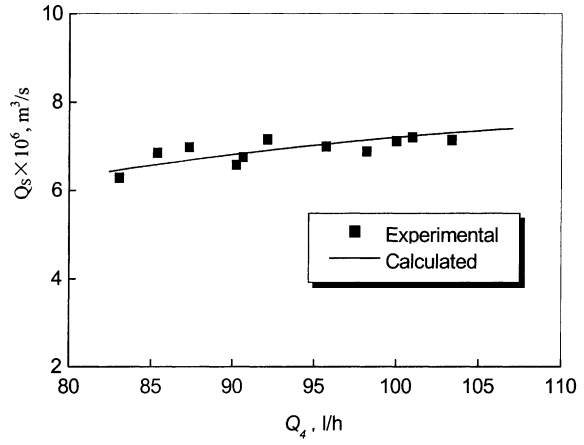

Fig. 7. Comparison of simulation data with experimental data when there is auxiliary liquid.

It can be seen from Eqs. (20) and (21) that when Q_E becomes small, the resistance coefficient ξ becomes great. This is because the particle-circulating rate increases when Q_E is reduced, and this leads to an increase of the friction resistance. Similarly, the friction coefficient will increase when there is auxiliary liquid because this increases the particle-circulating rate, leading to the growth of ξ.

3.5.2. Verification of model

In Figs. 6 and 7, the simulated results from the mathematical models have been compared with the experimental data with and without the auxiliary liquid. As illustrated in the figures, the model shows a satisfactory agreement with the experimental data.

4. Conclusions

1. The application of the auxiliary liquid can effectively regulate the particle-circulating rate in the liquid–solid circulating moving bed reactor. The auxiliary liquid flow III has the highest efficiency and is the best way of regulation for the particle transport.
2. The particle-circulating rate depends on the driving flowrate and the liquid flowrate in the lower conduit. The increase of driving flowrate and the decrease of the liquid flowrate in the lower conduit will increase the particle-circulating rate.
3. The mathematical transport model based on the mass, momentum and energy balances in the suction chamber is applicable and can be used to simulate the transport process with or without auxiliary liquid.

Acknowledgements

This work was funded by SIONPEC.

References

[1] M. Han, Y. Jin, J. Wang, et al., CN. 1,223,899A (1999).
[2] H.A. Boucher, et al., Alkylation of aromatic molecules using a silica–alumina catalyst derived from zeolite, US Patent 4,570,027, (1986).
[3] J.A. Kocal, Detergent alkylation process using a fluorided silica–alumina, US Patent 5,196,574, (1993).
[4] L.H. Slaugh, Alkylation of benzene compounds with detergent range olefins, US Patent 4,358,628 (1982).
[5] J.L.B. Tejero, B. De Monte, et al., Alkylation of aromatic hydrocarbons, US Patent 5,157,158 (1992).
[6] G.E. Seridde, Process for alkylating aromatic hydrocarbons and catalyst therefor, US Patent 3,992,467 (1976).
[7] L.B. Zinner, K. Zinner, M. Ishige, A.S. Araujo, Catalytic activity of lanthanide-doped Y zeolite on the alkylation of benzene with 1-dodecene model reaction, J. Alloys Comp. 193 (1993) 65–67.
[8] B.V. Vora, P.R. Pujado, T. Imai, T.R. Fritsch, Recent advances in the production of detergent olefins and linear alkylbenzenes, Tenside Surf. Det. 28 (4) (1991) 287–294.
[9] B. Vora, et al., Production of detergent olefins and linear alkylbenzenes, Chem. Ind. 19 (3) (1990) 187–191.
[10] B.V. Vora, Darien, P.R. Cottrell, Arlington heights, process for the production of alkylaromatic hydrocarbons using solid catalysts, US Patent 5,012,021 (1991).
[11] L.B. Young, Preparation of 2-phenylalkanes, US Patent 4,301,317 (1981).
[12] J.L.B. Tejero, B. de Algeciras. Alkylation of aromatic hydrocarbons in fixed bed catalytic process. US Patent 5,146,026A (1989).
[13] J.L.B. Tejero, B. de Algeciras. Alkylation of aromatic hydrocarbons, US Patent 5,157,158A (1991).
[14] H. Lu. Theory and Application of the Technology of Jet Pumps, Hydroelectric Press, Beijing, 1989, 52–78.